Johann Radon Institute for
Computational and Applied Mathematics
Austrian Academy of Sciences (ÖAW)

On the robustness of hierarchical multilevel splittings for discontinuous Galerkin rotated bilinear FE problems

I. Georgiev, J. Kraus, S. Margenov

RICAM-Report 2008-09

On the robustness of hierarchical multilevel splittings for discontinuous Galerkin rotated bilinear FE problems

I. Georgiev[*‡] J. Kraus[†] S. Margenov[‡]

Abstract

In this paper we present a new framework for multilevel preconditioning of large sparse systems of linear algebraic equations arising from the interior penalty discontinuous Galerkin approximation of second-order elliptic boundary value problems. Though the focus is on a particular family of rotated bilinear non-conforming (Rannacher-Turek) finite elements in two space dimensions (2D) the proposed rather general setting is neither limited to this particular choice of elements nor to 2D problems

Under the assumption that the finest partition is a result of multilevel refinement of a given coarse mesh, we develop a novel concept for the hierarchical splitting of the unknowns. Next we show how the constant in the strengthened Cauchy-Bunyakowski-Schwarz (CBS) inequality can be estimated locally in this setting. Two basic problems are studied: the scalar elliptic equation and the Lamé system of linear elasticity. This part of the presented theoretical results is in the spirit of algebraic multilevel iteration (AMLI) methods.

One innovative contribution of this work is the construction of robust methods for problems with large jumps (several orders of magnitude) in the PDE coefficients that can only be resolved on the finest finite element mesh. In the well-established theory of hierarchical basis multilevel methods one basic assumption is that the PDE coefficients are smooth functions on the elements of the coarsest mesh partition. The presented numerical study of the CBS constant shows a well expressed robustness of the developed hierarchical multilevel splitting with respect to coefficient jumps between elements on the finest mesh.

KEY WORDS: Discontinuous Galerkin methods, Rannacher-Turek finite elements, multilevel preconditioning, hierarchical basis, CBS constant.

1 Introduction

Optimal order algebraic multilevel iteration (AMLI) preconditioners based on recursive application of two-level finite element (FE) methods have been introduced and originally analyzed in context of linear conforming elements, see e.g., [4, 5]. The construction follows the natural hierarchical splitting using that the FE spaces corresponding to two successive mesh refinements are nested. The key role in the derivation of optimal convergence rate estimates plays the constant γ in the strengthened

[*]Institute of Mathematics and Informatics, Bulgarian Academy of Sciences, Acad. G. Bonchev Bl. 8, 1113 Sofia, Bulgaria, john@parallel.bas.bg

[†]Johann Radon Institute for Computational and Applied Mathematics, Austrian Academy of Sciences, Altenberger Strasse 69, A-4040 Linz, Austria, johannes.kraus@oeaw.ac.at

[‡]Institute for Parallel Processing, Bulgarian Academy of Sciences, Acad. G. Bonchev Bl. 25A, 1113 Sofia, Bulgaria, {john, margenov}@parallel.bas.bg

CBS inequality, associated with the angle between the two subspaces of the hierarchical splitting. It turns out that existence only of a uniform estimate for this constant is not enough, therefore, accurate quantitative bounds for γ are required as well. More precisely, the value of the upper bound for $\gamma \in (0, 1)$ is a part of the construction of the multilevel extension of the related two-level method.

More recently, optimal order AMLI methods related to Crouzeix-Raviart and Rannacher-Turek non-conforming finite elements have also been developed [6, 7, 15, 16, 21]. An important point to make is that in the case of non-conforming elements the finite element spaces corresponding to two successive levels of mesh refinement are not nested in general. To handle this, a proper two-level basis is required. The currently developed multilevel methods for non-conforming elements are in the spirit of the standard (linear) and non-linear AMLI methods for so called "First reduce" (FR) and "Differences and aggregates" (DA) hierarchical splittings.

In this paper we address AMLI preconditioners for linear algebraic systems obtained from interior penalty discontinuous Galerkin (IP-DG) finite element methods. In the case of scalar self-adjoint elliptic problems, the related stiffness matrix is symmetric and positive definite. Let us note that this is a special case of a more general class of DG schemes for second-order elliptic problems (see, e.g. [3, 9, 13]). Among the advantages of DG methods is that they are locally conservative which is of a principle importance for problems with strongly jumping coefficients. There are cited some first works on efficient solution methods for DG-FEM systems [8, 10, 11, 17].

Following the two-level approach from [10], a new class of AMLI methods for the resulting graph-Laplacian systems was introduced in [24]. The obtained optimal complexity results are applicable to a rather general setting of IP-DG problems. In [22, 23] novel AMLI preconditioners were studied for DG-FE discretization with conforming elements of 2D and 3D elliptic problems. In all these cases new concepts of local matrices are introduced to substitute the standard element stiffness matrices in the FEM assembling procedure. This idea is further developed and enriched in the present paper.

Two basic elliptic problems are studied in this article. The proposed constructions are first implemented to the case of a scalar equation. The next part of the study concerns the Lamé equations of linear elasticity. In the case of a nearly incompressible material the Q1P0 element using a conforming bilinear FEM approximation of the displacements and a piecewise constant approximation of the "pressure" is not quite stable. This phenomena is known as locking and typically appears in case of lower-order FEM. The Rannacher-Turek rotated bi/tri-linear elements were introduced for the Stokes problem [25] in combination with piecewise constant pressures. However, for the elasticity problem they are still not stable, a difficulty that has been overcome by Hansbo and Larson who introduced a locking-free DG-FEM approximation [18]. The presented generalized hierarchical basis for the related discrete problem is the core of a robust AMLI preconditioned iterative solution method. The construction is applied to the symmetric and positive definite stiffness matrix obtained after local elimination (reduced integration) of the pressure unknowns.

The commonly known theory of the optimal order solution methods for FEM elliptic systems is restricted to the case of coefficient jumps which are aligned with the coarse(st) geometric splitting. Such assumptions are usually made in the case of multilevel, multigrid and domain decomposition methods. There are many numerical tests confirming that the convergence of the related methods deteriorates if this condition is violated. At the same time, there are a lot of (multiscale and multiphysics) models of strongly heterogeneous media where the strong coefficient jumps are resolved on the finest level of the mesh. Such problems are recently referred to as "high frequency and high contrast". In the last part of this paper we show some pioneering results for such problems demonstrating the achieved robustness for classes of problems with extremely rough coefficients. Stochastically independent uniformly distributed random values of the diffusion coefficient (elasticity modulus) are used to set the configuration of the test problems.

2 Rannacher-Turek finite elements

Non-conforming rotated multilinear finite elements were introduced by Rannacher and Turek [25] as a class of simple elements for stable discretization of the Stokes problem. Let $\mathcal{T}$ be a regular decomposition of the domain $\Omega \subset \mathbb{R}^2$ into quadrilaterals denoted by T. The square $[-1,1]^2$ is used as a reference element $\hat{T}$ to define the isoparametric rotated bilinear element $T \in \mathcal{T}$. Let $\Psi_T : \hat{T} \to T$ be the corresponding bilinear bijective transformation. We set

$$Q_1(T) := \{q \circ \Psi_T^{-1} : q \in \text{span}\{1, x_1, x_2, x_1^2 - x_2^2\}\}.$$

For defining the corresponding local interpolation operators let us denote by Γ^i the faces of the element and by $\mathbf{m}^i$ the midpoints of the faces. There are natural sets of nodal functionals:

a) mean value continuity symbolized by the nodal functional $F^a_{\Gamma^i}(\mathbf{v}) = |\Gamma^i|^{-1} \displaystyle\int_{\Gamma^i} \mathbf{v} d\Gamma^i$.

b) midpoint continuity symbolized by the nodal functional $F^b_{\Gamma^i}(\mathbf{v}) = \mathbf{v}(\mathbf{m}^i)$.

The corresponding finite element spaces are

$$\begin{aligned} \mathbf{W}_h^{a/b} \quad := \quad & \Big\{ \mathbf{v} \in [L_2(\Omega)]^d : \mathbf{v} \in Q_1(T)\ \forall T \in \mathcal{T}, \mathbf{v} \text{ is continuous w.r.t.} \\ & \text{all the functionals } F^{a/b}_{\Gamma^i}, \text{ and } F^{a/b}_{\Gamma^i} = 0 \text{ if } \Gamma^i \subset \partial\Omega_D \Big\}, \end{aligned}$$

(where $d = 1$ for the scalar elliptic problem and $d = 2$ for the elasticity problem, respectively) and

$$L_h := \{q_h \in L_2(\Omega) : q_h|_T \in P_0\ \forall T \in \mathcal{T}\},$$

where P_0 is the space of constants. In [25] it is shown that $\mathbf{W}_h^a$ is less sensitive to mesh distortion than $\mathbf{W}_h^b$ when solving the Stokes problem, but that both are stable with respect to the Babuska-Brezzi condition. The space $\mathbf{W}_h^a$ is also more natural for the DG formulation.

3 Discontinuous Galerkin FE approximation of a scalar second-order elliptic problem

Consider a second-order elliptic problem on a polygonal domain $\Omega \subset R^2$:

$$\begin{aligned} -\nabla \cdot (a(x)\nabla u) &= f(x) \quad \text{in } \Omega, \\ u(x) &= 0 \quad \text{on } \Gamma_D, \\ a\nabla u \cdot \mathbf{n} &= 0 \quad \text{on } \Gamma_N. \end{aligned} \tag{1}$$

Here $\mathbf{n}$ is the exterior unit normal vector on Γ_N. The boundary is assumed to be decomposed into two disjoint parts Γ_D and Γ_N, $\Gamma_D \cap \Gamma_N = \emptyset$. For the formulation below we shall need the existence of the traces of u and $a\nabla u \cdot \mathbf{n}$ on certain interfaces in Ω. Thus, the solution u is assumed to have the required regularity. To simplify our exposition we assume that the set Γ_D is not empty and its measure in nonzero.

We assume also that the partition $\mathcal{T}$ is quasi uniform and regular. For each finite element we denote by h_T its size and further $h = \max_{T \in \mathcal{T}} h_T$. Let $e = \overline{T}_1 \cap \overline{T}_2$ be the interface of two adjacent elements T_1, T_2. The set of all such interfaces is denoted by $\mathcal{E}_I$, note that these interfaces are inside Ω. Further, $\mathcal{E}_D$ and $\mathcal{E}_N$ will be the faces of finite elements on the boundary Γ_D and Γ_N, respectively. Finally, $\mathcal{E}$ will be the set of all faces:

$$\mathcal{E} = \mathcal{E}_I \cup \mathcal{E}_D \cup \mathcal{E}_N. \tag{2}$$

On the partition $\mathcal{T}$ we consider the finite element space $\mathbf{W}_h^a$ (with $d = 1$). For each $e = \bar{T}_1 \cap \bar{T}_2 \in \mathcal{E}_I$ we define the jump $[\![v]\!]$ of any function $v \in \mathbf{W}_h^a$ as the vector

$$[\![v]\!]_e := \begin{cases} v|_{T_1} \cdot \mathbf{n}_1 + v|_{T_2} \cdot \mathbf{n}_2, & e = \bar{T}_1 \cap \bar{T}_2, \text{ i.e. } e \in \mathcal{E}_I, \\ v|_{T_1} \cdot \mathbf{n}_1, & e = \bar{T}_1 \cap \Gamma_D, \text{ i.e. } e \in \mathcal{E} \setminus \mathcal{E}_I. \end{cases}$$

Here $\mathbf{n}_1$ and $\mathbf{n}_2$ are the external unit vectors to T_1 and T_2, respectively.

We shall also need the following notation for the average value of the traces of a vector function $\mathbf{v} \in \mathbf{W}_h^a$ on $e = \bar{T}_1 \cap \bar{T}_2$

$$\{\mathbf{v}\}|_e := \begin{cases} \frac{1}{2}(\mathbf{v}|_{T_1} + \mathbf{v}|_{T_2}) & e = \bar{T}_1 \cap \bar{T}_2, \text{ i.e. } e \in \mathcal{E}_I, \\ \mathbf{v}|_{T_1}, & e = \bar{T}_1 \cap \Gamma_D, \text{ i.e. } e \in \mathcal{E} \setminus \mathcal{E}_I \end{cases}$$

and the piecewise constant function $h_{\mathcal{E}}$ defined on $\mathcal{E}$ as

$$h_{\mathcal{E}} = h_{\mathcal{E}}(x) = |e|, \quad \text{for } x \in e \in \mathcal{E}.$$

Further we define

$$(a\nabla v, \nabla v)_{\mathcal{T}} := \sum_{T \in \mathcal{T}} \int_T a\nabla u \, \nabla v \, dx, \quad \left\langle h_{\mathcal{E}}^{-1} [\![u]\!], [\![v]\!] \right\rangle_{\mathcal{E} \cup \mathcal{E}_D} := \sum_{e \in \mathcal{E} \cup \mathcal{E}_D} \int_e h_{\mathcal{E}}^{-1} [\![u]\!] \cdot [\![v]\!] ds.$$

We shall use also the mesh dependent norm

$$|||v|||^2 = (a\nabla v, \nabla v)_{\mathcal{T}} + \alpha \left\langle h_{\mathcal{E}}^{-1} [\![v]\!], [\![v]\!] \right\rangle_{\mathcal{E} \cup \mathcal{E}_D}. \tag{3}$$

In this study we consider the following symmetric interior penalty discontinuous Galerkin finite element method (see, e.g. [3]): Find $u_h \in \mathbf{W}_h^a$ such that

$$\mathcal{A}(u_h, v) = \mathcal{L}(v), \quad \forall \, v \in \mathbf{W}_h^a, \tag{4}$$

where

$$\begin{aligned} \mathcal{A}(u_h, v) \equiv \quad & (a\nabla u_h, \nabla v)_{\mathcal{T}} + \alpha \left\langle {h_{\mathcal{E}}}^{-1} [\![u_h]\!], [\![v]\!] \right\rangle_{\mathcal{E} \cup \mathcal{E}_D} \\ & - \langle \{a\nabla u_h\}, [\![v]\!] \rangle_{\mathcal{E} \cup \mathcal{E}_D} - \langle [\![u_h]\!], \{a\nabla v\} \rangle_{\mathcal{E} \cup \mathcal{E}_D} \end{aligned} \tag{5}$$

and

$$\mathcal{L}(v) = (f, v).$$

We summarize the main results regarding the discontinuous Galerkin method (4) in the following lemma (see, e.g. [3]).

Lemma 3.1 *Assume that the finite element partition $\mathcal{T}$ is regular and locally quasi-uniform. Then the bilinear form $\mathcal{A}(\cdot, \cdot)$ defined by (5) is coercive and bounded in $\mathbf{W}_h^a$ equipped with the norm (3) for any sufficiently large $\alpha > 0$ and the discontinuous Galerkin method (4) has unique solution.*

The global stiffness matrix related to the bilinear form (5) can be assembled from the small-sized local face stiffness matrices

$$A = \sum_{e \in \mathcal{E}} A_e.$$

The matrix A_e is related to the local bilinear form associated with the face e, and has the form

$$\begin{aligned} \mathcal{A}_e(u_h, v) \equiv \quad & \frac{1}{4} \left((a\nabla u_h, \nabla v)_{T^+} + (a\nabla u_h, \nabla v)_{T^-} \right) + \alpha \left\langle {h_{\mathcal{E}}}^{-1} [\![u_h]\!], [\![v]\!] \right\rangle_{\mathcal{E} \cup \mathcal{E}_D} \\ & - \langle \{a\nabla u_h\}, [\![v]\!] \rangle_{\mathcal{E} \cup \mathcal{E}_D} - \langle [\![u_h]\!], \{a\nabla v\} \rangle_{\mathcal{E} \cup \mathcal{E}_D}. \end{aligned}$$

In the model case of a mesh of square elements the matrices corresponding to the single contributions of horizontal and vertical (interior) faces have the representation

$$A_e^{\rm h} = A_{e,0}^{\rm h} + \alpha A_{e,1}^{\rm h}, \tag{6}$$
$$A_e^{\rm v} = A_{e,0}^{\rm v} + \alpha A_{e,1}^{\rm v}. \tag{7}$$

The matrix terms from the r.h.s. of (6) can be writtenin the form

$$A_{e,0}^{\rm h} = \frac{1}{8}\begin{bmatrix} 5k^+ & -3k^+ & 3k^+ & k^+ & 0 & -6k^+ & 0 & 0 \\ -3k^+ & 5k^+ & -k^+ & -3k^+ & 0 & 2k^+ & 0 & 0 \\ 3k^+ & -k^+ & -15k^+ & 3k^+ & -6k^- & 10(k^+ + k^-) & 2k^- & -6k^- \\ k^+ & -3k^+ & 3k^+ & 5k^+ & 0 & -6k^+ & 0 & 0 \\ 0 & 0 & -6k^- & 0 & 5k^- & 3k^- & -3k^- & k^- \\ -6k^+ & 2k^+ & 10(k^+ + k^-) & -6k^+ & 3k^- & -15k^- & -k^- & 3k^- \\ 0 & 0 & 2k^- & 0 & -3k^- & -k^- & 5k^- & -3k^- \\ 0 & 0 & -6k^- & 0 & k^- & 3k^- & -3k^- & 5k^- \end{bmatrix},$$

$$A_{e,1}^{\rm h} = \frac{1}{240}\begin{bmatrix} 23 & -3 & -3 & -17 & -23 & 3 & 3 & 17 \\ -3 & 3 & 3 & -3 & 3 & -3 & -3 & 3 \\ -3 & 3 & 243 & -3 & 3 & -243 & -3 & 3 \\ -17 & -3 & -3 & 23 & 17 & 3 & 3 & -23 \\ -23 & 3 & 3 & 17 & 23 & -3 & -3 & -17 \\ 3 & -3 & -243 & 3 & -3 & 243 & 3 & -3 \\ 3 & -3 & -3 & 3 & -3 & 3 & 3 & -3 \\ 17 & 3 & 3 & -23 & -17 & -3 & -3 & 23 \end{bmatrix}.$$

Here the isotropic coefficient matrix $a = a(T)$ is defined by

$$a(T^{\pm}) = k^{\pm}\begin{bmatrix} 1 & 0 \\ 0 & 1 \end{bmatrix}.$$

The vertical face matrix$A_e^{\rm v}$ is obtained from $A_e^{\rm h}$ via the following permutation[1] of rows and columns if the mesh is composed of square elements:

$$A_e^{\rm v} = S_{\rm h,v}^t A_e^{\rm h} S_{\rm h,v},$$

where

$$(S_{\rm h,v})_{i,j} = \begin{cases} 1 & \text{if} \quad j = \mathbf{s}_i \\ 0 & \text{else} \end{cases}, \tag{8}$$
$$\mathbf{s} = (2,1,4,3,6,5,8,7)^t$$

and the numbering of nodes belonging to horizontal and vertical faces is as shown in Figure 1.

Remark 3.1 For the considered particular case of a mesh of square elements the analysis of the stabilization parameter shows that when $k^+ = k^-$ the condition of Lemma 3.1 is satisfied for $\alpha > \dfrac{\sqrt{23329} - 127}{8} \approx 3.22$.

[1] In all different cases, the same latter S stands for the permutation matrix.

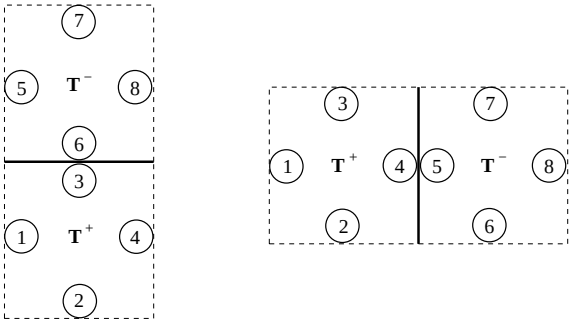

Figure 1: Degrees of freedom of face matrices: horizontal face (left) and vertical face (right)

4 DG approximation of the Lamé linear elasticity problem

Let us consider the mixed formulation of the linear elasticity problem: Find the displacements $\mathbf{u} = [u_i]_{i=1}^2$ and the "pressure" p such that

$$\begin{aligned} -\nabla.(2\mu\varepsilon(\mathbf{u}) - p\mathbf{I}) &= \mathbf{f} \text{ in } \Omega, \\ \frac{1}{\lambda}p + \nabla.\mathbf{u} &= 0 \text{ in } \Omega, \\ \mathbf{u} &= 0 \text{ on } \Gamma_D, \\ (2\mu\varepsilon(\mathbf{u}) - p\mathbf{I}).\mathbf{n} &= \mathbf{h} \text{ on } \Gamma_N. \end{aligned} \tag{9}$$

Here λ and μ are the Lamé coefficients, satisfying the inequalities $0 < \mu_1 < \mu < \mu_2$ and $0 < \lambda < \infty$, and $\varepsilon(\mathbf{u}) = [\varepsilon_{ij}(\mathbf{u})]_{i,j=1}^2$ is the strain tensor with components

$$\varepsilon_{ij}(\mathbf{u}) = \frac{1}{2}\left(\frac{\partial u_i}{\partial x_j} + \frac{\partial u_j}{\partial x_i}\right).$$

Furthermore, $\mathbf{I} = [\delta_{ij}]_{i,j=1}^2$ with $\delta_{ij} = 1$ if $i = j$ and $\delta_{ij} = 0$ if $i \neq j$, $\mathbf{f}$ and $\mathbf{h}$ are given loads, and $\mathbf{n}$ is the outward unit normal to Γ_N. In terms of the modulus of elasticity, E, and Poisson's ratio, ν, we have, in the case of plane strain, that $\lambda = E\nu/((1+\nu)(1-2\nu))$ and $\mu = E/(2(1+\nu))$. Incompressible behavior is obtained as the parameter $\lambda \to \infty$, i.e., as $\nu \to 1/2$. In such a case standard (low-order) FE methods will lock. In the general case RT elements cannot control the rigid body rotations, which leads to instability, see Huges [19]. In [18] Hansbo and Larson presented a special discontinuous Galerkin framework for RT elements which leads to a stable discretization of (9).

We again assume that the partition $\mathcal{T}$ of Ω is quasi uniform and regular. Here with each face $e \in \mathcal{E}$ (see (2)) we associate a fixed unit normal $\mathbf{n}$ such that for faces on the boundary $\mathbf{n}$ is the exterior unit normal. We denote here the jump of a vector function $\mathbf{v} \in \mathbf{W}_h^a$ at a given face e by $[\![\mathbf{v}]\!] = \mathbf{v}^+ - \mathbf{v}^-$ for $e \in \mathcal{E}_I$ and $[\![\mathbf{v}]\!] = \mathbf{v}^+$ for $e \in \mathcal{E}_D$, and the average $\{\mathbf{v}\} = (\mathbf{v}^+ + \mathbf{v}^-)/2$ for $e \in \mathcal{E}_I$ and $\{\mathbf{v}\} = \mathbf{v}^+$ for $e \in \mathcal{E}_D$, where $\mathbf{v}^\pm = \lim_{\epsilon \downarrow 0} \mathbf{v}(\mathbf{x} \mp \epsilon\mathbf{n})$ with $\mathbf{x} \in e$. The discontinuous Galerkin method for the problem (9) reads (see [18]): Find $(\mathbf{u}_h, p_h) \in \mathbf{W}_h^a \times L_h$ such that

$$\mathcal{A}(\mathbf{u}_h, \mathbf{v}, p_h, q) = \mathcal{L}(\mathbf{v}) \text{ for all } (\mathbf{v}, q) \in \mathbf{W}_h^a \times L_h, \tag{10}$$

The bilinear form

$$\mathcal{A}(\mathbf{u}_h, p_h, \mathbf{v}, q) \equiv a(\mathbf{u}_h, \mathbf{v}) + b(\mathbf{u}_h, q) + b(\mathbf{v}, p_h) + c(p_h, q) \tag{11}$$

is defined as follows:

$$
\begin{aligned}
a(\mathbf{u}_h, \mathbf{v}) \;\; := \;\; & \sum_{T\in\mathcal{T}} (2\mu\varepsilon(\mathbf{u}_h), \varepsilon(\mathbf{v}))_T \\
& - \sum_{e\in\mathcal{E}_I\cup\mathcal{E}_D} \langle\{2\mu\varepsilon(\mathbf{u}_h)\cdot\mathbf{n}\}, [\![\mathbf{v}]\!]\rangle_e + \langle\{2\mu\varepsilon(\mathbf{v})\cdot\mathbf{n}\}, [\![\mathbf{u}_h]\!]\rangle_e \\
& + 2\mu\alpha \sum_{e\in\mathcal{E}_I\cup\mathcal{E}_D} \left\langle h_{\mathcal{E}}^{-1} [\![\mathbf{u}_h]\!], [\![\mathbf{v}]\!]\right\rangle_e ,
\end{aligned}
$$

$$
b(\mathbf{v}, q) := -\sum_{T\in\mathcal{T}} (q, \nabla\cdot\mathbf{v})_T + \sum_{e\in\mathcal{E}_I\cup\mathcal{E}_D} \langle\{q\}, [\![\mathbf{v}\cdot\mathbf{n}]\!]\rangle_e ,
$$

$$
c(p_h, q) := -\sum_{T\in\mathcal{T}} (\lambda^{-1} p_h, q)_T,
$$

and the linear functional is given by

$$
\mathcal{L}(\mathbf{v}) := \sum_{T\in\mathcal{T}} (\mathbf{f}, \mathbf{v})_T + \sum_{e\in\mathcal{E}_N} \langle \mathbf{h}, \mathbf{v}\rangle_e .
$$

Here $(\mathbf{v}, \mathbf{w})_T = \int_T \sum_{ij} \mathbf{v}_{ij}\mathbf{w}_{ij}$, for 2-tensors $\mathbf{v}, \mathbf{w}$; $\langle \mathbf{v}, \mathbf{w}\rangle_e = \int_e \sum_i \mathbf{v}_i\mathbf{w}_i$, for vectors $\mathbf{v}, \mathbf{w}$. Note that the incompressible limit $\lambda \to \infty$ corresponds to $c(\cdot,\cdot) = 0$. We shall use the following mesh depending energy norm

$$
|||v|||^2 = \sum_{T\in\mathcal{T}} (2\mu\varepsilon(\mathbf{v}), \varepsilon(\mathbf{v}))_T + \sum_{e\in\mathcal{E}_I\cup\mathcal{E}_D} \left\langle h_{\mathcal{E}}^{-1} [\![\mathbf{v}]\!], [\![\mathbf{v}]\!]\right\rangle_e ,
$$

and the norm on L_h,

$$
||q||_{L_h}^2 = \sum_{T\in\mathcal{T}} ||q||_{L^2(T)}^2 .
$$

In the following lemma we summarize the main results regarding the DG method (10), see [18].

Lemma 4.1 *Assume that the finite element partition $\mathcal{T}$ is regular and locally quasi uniform. Then the following stability conditions are satisfied uniformly with respect to the Poisson ratio $\nu \in [0, \frac{1}{2})$:*

1. *There is a constant $\alpha \geq \alpha_0 > 0$ such that*

$$
\alpha\, |||v||| \leq a(\mathbf{v}, \mathbf{v}) \;\; \textit{for all} \;\; \mathbf{v} \in \mathbf{W}_h^a;
$$

2. *There is a constant $\beta \geq \beta_0 > 0$ such that*

$$
\beta \leq \inf_{q\in L_h} \sup_{\mathbf{v}\in\mathbf{W}_h^a} \frac{b(\mathbf{v}, q)}{|||v|||\, ||q||_{L_h}};
$$

and the discontinuous Galerkin method (10) has unique solution.

As the consequence of this lemma we have locking-free error estimates for the IP-DG approximation. The indefinite stiffness matrix K corresponding to the bilinear form (11) can be represented in the following 2×2 block form

$$
K = \left[\begin{array}{cc} A & B \\ B^t & C \end{array} \right]. \tag{12}
$$

The matrix K can be assembled from so-called face-stiffness matrices related to the local bilinear form associated with faces. In what follows, possible coefficient jumps across the faces are also included (see [11]):

$$\mathcal{A}_e(\mathbf{u}_h, p_h, \mathbf{v}, q) \equiv a_e(\mathbf{u}_h, \mathbf{v}) + b_e(\mathbf{u}_h, q) + b_e(\mathbf{v}, p_h) + c_e(p_h, q)$$

and

$$\begin{aligned} a_e(\mathbf{u}_h, \mathbf{v}) &= \frac{1}{4}\left((2\mu^+\varepsilon(\mathbf{u}_h), \varepsilon(\mathbf{v}))_{T^+} + (2\mu^-\varepsilon(\mathbf{u}_h), \varepsilon(\mathbf{v}))_{T^-}\right) \\ &\quad - \left(\langle\{2\mu\varepsilon\mathbf{u}_h)\cdot\mathbf{n}\}, [\![\mathbf{v}]\!]\rangle_e + \langle\{2\mu\varepsilon\mathbf{v})\cdot\mathbf{n}\}, [\![\mathbf{u}_h]\!]\rangle_e\right) \\ &\quad + (\mu^+ + \mu^-)\alpha\left\langle h_{\mathcal{E}}^{-1}[\![\mathbf{u}_h]\!], [\![\mathbf{v}]\!]\right\rangle_e, \\ b_e(\mathbf{v}, q) &= -\frac{1}{4}\left((q, \nabla\cdot\mathbf{v})_{T^+} + (q, \nabla\cdot\mathbf{v})_{T^-}\right) + \langle\{q\}, [\![\mathbf{v}\cdot\mathbf{n}]\!]\rangle_e, \\ c_e(p_h, q) &= -\frac{1}{4}\left(\left(\frac{1}{\lambda^+}p_h, q\right)_{T^+} + \left(\frac{1}{\lambda^-}p_h, q\right)_{T^-}\right). \end{aligned}$$

The submatrix C in (12) corresponding to the "pressures" is diagonal and hence we can eliminate these unknowns exactly. Then we end up with a symmetric and positive definite stiffness matrix $\widetilde{K} = A - BC^{-1}B^t$. In the model case of a mesh of square elements the single contributions to $\widetilde{K}$ of horizontal and vertical (interior) faces are the following:

$$A_e^{\mathrm{h}} = A_{e,0}^{\mathrm{h}} + \alpha A_{e,1}^{\mathrm{h}} \tag{13}$$

$$A_e^{\mathrm{v}} = A_{e,0}^{\mathrm{v}} + \alpha A_{e,1}^{\mathrm{v}}. \tag{14}$$

The matrix $A_{e,0}^{\mathrm{h}}$ is written in 2×2 block form

$$A_{e,0}^{\mathrm{h}} = \frac{1}{16}\begin{bmatrix} A_{e,0}^{\mathrm{h},11} & A_{e,0}^{\mathrm{h},12} \\ A_{e,0}^{\mathrm{h},21} & A_{e,0}^{\mathrm{h},22} \end{bmatrix},$$

where

$$A_{e,0}^{\mathrm{h},11} = \begin{bmatrix} 17\mu^+ & -9\mu^+ & 3\mu^+ & \mu^+ & 0 & -12\mu^+ & 0 & 0 \\ -9\mu^+ & 13\mu^+ & \mu^+ & -9\mu^+ & 0 & 4\mu^+ & 0 & 0 \\ 3\mu^+ & \mu^+ & -27\mu^+ & 3\mu^+ & -12\mu^- & 20(\mu^-+\mu^+) & 4\mu^- & -12\mu^- \\ \mu^+ & -9\mu^+ & 3\mu^+ & 17\mu^+ & 0 & -12\mu^+ & 0 & 0 \\ 0 & 0 & -12\mu^- & 0 & 17\mu^- & 3\mu^- & -9\mu^- & \mu^- \\ -12\mu^+ & 4\mu^+ & 20(\mu^-+\mu^+) & -12\mu^+ & 3\mu^- & -27\mu^- & \mu^- & 3\mu^- \\ 0 & 0 & 4\mu^- & 0 & -9\mu^- & \mu^- & 13\mu^- & -9\mu^- \\ 0 & 0 & -12\mu^- & 0 & \mu^- & 3\mu^- & -9\mu^- & 17\mu^- \end{bmatrix}$$

$$+ \begin{bmatrix} 4\lambda^+ & 0 & 0 & -4\lambda^+ & 0 & 0 & 0 & 0 \\ 0 & 0 & 0 & 0 & 0 & 0 & 0 & 0 \\ 0 & 0 & 0 & 0 & 0 & 0 & 0 & 0 \\ -4\lambda^+ & 0 & 0 & 4\lambda^+ & 0 & 0 & 0 & 0 \\ 0 & 0 & 0 & 0 & 4\lambda^- & 0 & 0 & -4\lambda^- \\ 0 & 0 & 0 & 0 & 0 & 0 & 0 & 0 \\ 0 & 0 & 0 & 0 & 0 & 0 & 0 & 0 \\ 0 & 0 & 0 & 0 & -4\lambda^- & 0 & 0 & 4\lambda^- \end{bmatrix},$$

$$A_{e,0}^{\mathrm{h},12} = \begin{bmatrix} 2\mu^+ & 4\lambda^+ - 2\mu^+ & 4\lambda^+ - 2\mu^+ & 2\mu^+ & 2\mu^- & -8\lambda^+ - 2\mu^- & -2\mu^- & 2\mu^- \\ 4\mu^+ & 0 & 0 & -4\mu^+ & 0 & 0 & 0 & 0 \\ 4\mu^+ & 0 & 0 & -4\mu^+ & 8\mu^- & 0 & 0 & -8\mu^- \\ -2\mu^+ & -4\lambda^+ + 2\mu^+ & -4\lambda^+ + 2\mu^+ & -2\mu^+ & -2\mu^- & 8\lambda^+ + 2\mu^- & 2\mu^- & -2\mu^- \\ -2\mu^+ & 2\mu^+ & 8\lambda^- + 2\mu^+ & -2\mu^+ & -2\mu^- & -4\lambda^- + 2\mu^- & -4\lambda^- + 2\mu^- & -2\mu^- \\ -8\mu^+ & 0 & 0 & 8\mu^+ & -4\mu^- & 0 & 0 & 4\mu^- \\ 0 & 0 & 0 & 0 & -4\mu^- & 0 & 0 & 4\mu^- \\ 2\mu^+ & -2\mu^+ & -8\lambda^- - 2\mu^+ & 2\mu^+ & 2\mu^- & 4\lambda^- - 2\mu^- & 4\lambda^- - 2\mu^- & 2\mu^- \end{bmatrix},$$

$$A_{e,0}^{\mathrm{h},21} = \left(A_{e,0}^{\mathrm{h},12}\right)^t,$$

$$A_{e,0}^{\mathrm{h},22} = \begin{bmatrix} 13\mu^+ & -9\mu^+ & 15\mu^+ & 5\mu^+ & 0 & -24\mu^+ & 0 & 0 \\ -9\mu^+ & 17\mu^+ & -7\mu^+ & -9\mu^+ & 0 & 8\mu^+ & 0 & 0 \\ 15\mu^+ & -7\mu^+ & -63\mu^+ & 15\mu^+ & -24\mu^- & 40(\mu^- + \mu^+) & 8\mu^- & -24\mu^- \\ 5\mu^+ & -9\mu^+ & 15\mu^+ & 13\mu^+ & 0 & -24\mu^+ & 0 & 0 \\ 0 & 0 & -24\mu^- & 0 & 13\mu^- & 15\mu^- & -9\mu^- & 5\mu^- \\ -24\mu^+ & 8\mu^+ & 40(\mu^- + \mu^+) & -24\mu^+ & 15\mu^- & -63\mu^- & -7\mu^- & 15\mu^- \\ 0 & 0 & 8\mu^- & 0 & -9\mu^- & -7\mu^- & 17\mu^- & -9\mu^- \\ 0 & 0 & -24\mu^- & 0 & 5\mu^- & 15\mu^- & -9\mu^- & 13\mu^- \end{bmatrix}$$

$$+ \begin{bmatrix} 0 & 0 & 0 & 0 & 0 & 0 & 0 & 0 \\ 0 & 4\lambda^+ & 4\lambda^+ & 0 & 0 & -8\lambda^+ & 0 & 0 \\ 0 & 4\lambda^+ & 16\lambda^- + 4\lambda^+ & 0 & 0 & -8(\lambda^- + \lambda^+) & -8\lambda^- & 0 \\ 0 & 0 & 0 & 0 & 0 & 0 & 0 & 0 \\ 0 & 0 & 0 & 0 & 0 & 0 & 0 & 0 \\ 0 & -8\lambda^+ & -8(\lambda^- + \lambda^+) & 0 & 0 & 4\lambda^- + 16\lambda^+ & 4\lambda^- & 0 \\ 0 & 0 & -8\lambda^- & 0 & 0 & 4\lambda^- & 4\lambda^- & 0 \\ 0 & 0 & 0 & 0 & 0 & 0 & 0 & 0 \end{bmatrix},$$

and

$$A_{e,1}^{\mathrm{h}} = \frac{\mu^+ + \mu^-}{240} \begin{bmatrix} A_{e,1}^{\mathrm{h},11} & \mathbf{0} \\ \mathbf{0} & A_{e,1}^{\mathrm{h},22} \end{bmatrix},$$

$$A_{e,1}^{\mathrm{h},11} = A_{e,1}^{\mathrm{h},22} = \begin{bmatrix} 23 & -3 & -3 & -17 & -23 & 3 & 3 & 17 \\ -3 & 3 & 3 & -3 & 3 & -3 & -3 & 3 \\ -3 & 3 & 243 & -3 & 3 & -243 & -3 & 3 \\ -17 & -3 & -3 & 23 & 17 & 3 & 3 & -23 \\ -23 & 3 & 3 & 17 & 23 & -3 & -3 & -17 \\ 3 & -3 & -243 & 3 & -3 & 243 & 3 & -3 \\ 3 & -3 & -3 & 3 & -3 & 3 & 3 & -3 \\ 17 & 3 & 3 & -23 & -17 & -3 & -3 & 23 \end{bmatrix}.$$

In order to deduce the face matrix for a vertical face (14) from (13) we note that the permutation (8) has to be applied to the x-displacement and to the y-displacement component separately, thereby taking into account that the role of x and y has to be interchanged, too. That is, the face matrix A_e^{v} for the vertical face is given by

$$A_e^{\mathrm{v}} = S_{\mathrm{h,v}}^t A_e^{\mathrm{h}} S_{\mathrm{h,v}}, \tag{15}$$

where

$$(S_{\mathrm{h,v}})_{i,j} = \begin{cases} 1 & \text{if} \quad j = \mathbf{s}_i \\ 0 & \text{else} \end{cases},$$
$$\mathbf{s} = (10, 9, 12, 11, 14, 13, 16, 15, 2, 1, 4, 3, 6, 5, 8, 7)^t$$

with respect to the component-by component ordering.

Remark 4.1 For the considered model case of a mesh of square elements the analysis of the stabilization parameter α shows that when $\lambda^+ = \lambda^-$ and $\mu^+ = \mu^-$ the stiffness matrix $\widetilde{K}$ is symmetric and positive definite for $\alpha \geq \alpha_0 = \dfrac{\sqrt{5689} - 37}{8} \approx 4.8$.

5 Splitting of the DG finite element spaces

The decomposition of the DG-FE space into a coarse space and its complementary space on the discrete (matrix) level is based on a (generalized) hierarchical basis transformation that can be defined locally, i.e., for so-called macro superelements. We will describe the procedure for the scalar elliptic problem in detail. A generalization to systems of partial differential equations, such as the Lamé system of linear elasticity, will be presented at the end of this section.

The first step in the construction is related to a splitting of the local bilinear form into the contributions associated with the single horizontal and vertical (interior) faces in the mesh (see (6) and (7)).

In the next step we define a general so-called superelement $g \in \mathcal{G}$, which is the union of all the degrees of freedom (DOF) associated with the four faces (two horizontal and two vertical faces) that share one vertex, see Figure 2. The characteristic macro superelement $G \in \mathcal{M}$ is then made

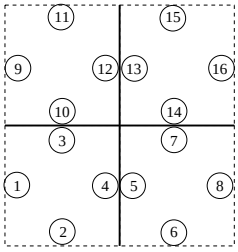

Figure 2: Superelement g composed of two horizontal and two vertical faces

up of four partly overlapping superelements as shown in Figure 3. Note that the construction of faces, superelements and macro superelements is such that the global stiffness matrix can always be assembled alternatively, in either way, of the respective local matrices, i.e.,

$$A = \sum_{e \in \mathcal{E}} A_e = \sum_{g \in \mathcal{G}} A_g = \sum_{G \in \mathcal{M}} A_G.$$

Due to the overlap of superelements the assembing of superelement matrices requires a proper scaling of the respective face contributions. For an interior superelement g the correct scaling factor is $1/2$,

i.e., $A_g = \sum_{e \subset g} \frac{1}{2} A_e$. The superelements can be associated with the vertices of the mesh, i.e., each vertex - intersection of (four interior) faces - defines one superelement and the coupling between the unknowns corresponding to different elements in a given superelement is due to the face matrices. The macro superelements finally cover the whole domain, i.e., the whole mesh, forming stripes of overlap with a width of one element, see Figure 4. The overlapping region (intersection) of all four superelements of a macro superelement is one element in its center, i.e., the element with the local DOF (respectively nodes) $1, 2, 3, 4$, as depicted in Figure 3. The DOF in the macro superelement G are divided into coarse DOF that belong to the corner elements – indicated by squares – and the remaining fine DOF – indicated by circles. As usual, the coarse DOF of a macro superelement form the DOF of a superelement on the next coarser level.

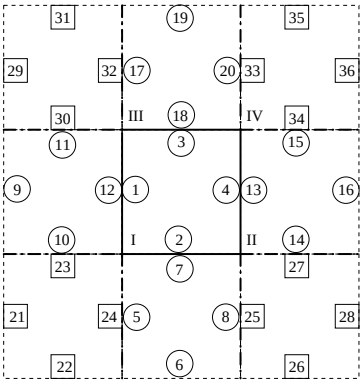

Figure 3: Macro superelement G: four overlapping superelements

The basic construction follows now from the standard approach, as it is used for conforming bilinear elements, if one associates nodes with elements. Hence, in the present context, we consider superelements g (instead of elements) in order to compose macro superelements G (instead of macro elements). Superelements produce overlapping (common) elements (instead of common nodes in the standard setting). Two "neighboring" macro superelements have three elements in common, see Figure 4 (instead of having three common nodes in the standard situation of conforming bilinear elements). The coarse mesh hierarchy is such that the DOF associated with every other element (in x- and every other element in y-direction) belong to the coarse level. Since all DOF of a given element are either "fine" or "coarse", the number of coarse DOF is always a multiple of four in the scalar case. The number of elements that contain the coarse DOF is approximately reduced by a factor 4 (for large meshes) and thus the coarsening ratio $\tau \approx 4$, see Figure 4. The macro superelement matrix associated with G is denoted by A_G; It is transformed into a hierarchical two-level basis via a local transformation

$$\hat{A}_G = J_G^t A_G J_G \tag{16}$$

where J_G has the form

$$J_G = \begin{bmatrix} I & P_G \\ 0 & I \end{bmatrix} \tag{17}$$

and P_G denotes some proper local interpolation matrix of size 20×16 (in the scalar case). Note that the local and global hierarchical bases, as presented here, do not involve so-called differences and

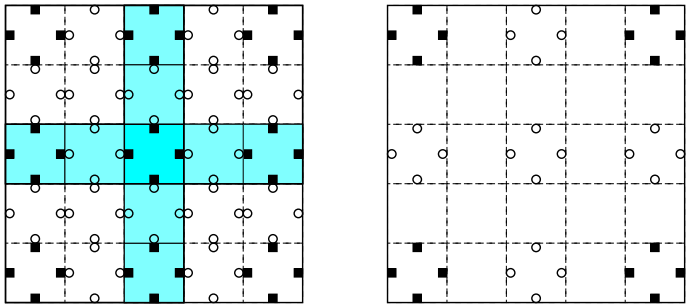

Figure 4: Coarsening and overlap of macro superelements

aggregates of nodal shape functions. As opposed to the latter construction, which has turned out to be useful for splitting certain non-conforming FE spaces in a proper way, see, e.g., [7, 16, 21], we stay within the framework of nested spaces here. In the following we give some examples of particular choices of the local transformation J_G, which define uniquely a global two-level splitting in each individual case.

In the first example we define J_G, as given by (17), by means of a local interpolation P_G that is based on simple averaging, i.e.,

$$P_G^{(1)} = \frac{1}{16} \begin{bmatrix} \mathbb{1} & \mathbb{1} & \mathbb{1} & \mathbb{1} \\ 2\mathbb{1} & 2\mathbb{1} & 0 & 0 \\ 2\mathbb{1} & 0 & 2\mathbb{1} & 0 \\ 0 & 2\mathbb{1} & 0 & 2\mathbb{1} \\ 0 & 0 & 2\mathbb{1} & 2\mathbb{1} \end{bmatrix}. \tag{18}$$

Here $\mathbb{1}$ denotes the 4×4 matrix of all ones. The resulting transformation we denote by $J_G^{(1)}$.

In the other examples we exploit a technique known as "First Reduce" approach, where we perform a so-called static condensation of the interior macro superelement DOF with local numbers $1, 2, 3, 4$, see Figure 3. After this reduction step we arrive at a (in the scalar case 32×32) local Schur complement

$$B_G = A_{G:22} - A_{G:21} A_{G:11}^{-1} A_{G:12}.$$

Here $A_{G:11}$ denotes the upper-left 4×4 submatrix that is associated with the interior DOF of G, which are subject to the elimination. This static condensation yields a local transformation into block diagonal form, i.e., a decoupling of the interior DOF from the remaining ones:

$$\begin{bmatrix} A_{G:11} & 0 \\ 0 & B_G \end{bmatrix} = \begin{bmatrix} I & 0 \\ -A_{G:21} A_{G:11}^{-1} & I \end{bmatrix} \begin{bmatrix} A_{G:11} & A_{G:12} \\ A_{G:21} & A_{G:22} \end{bmatrix} \begin{bmatrix} I & -A_{G:11}^{-1} A_{G:12} \\ 0 & I \end{bmatrix}$$

Since there is no overlap of the central element (no common interior DOF) of different macro superelements G, the exact elimination of interior unknowns in the global system can be done locally, i.e., for each macro superelement separately. For the transformation of the local matrices B_G associated with the reduced macro superelements, as depicted in Figure 5, the interpolation can be based on averaging again. This results in the same lower (in the scalar case 16×16) square submatrix as in the

interpolation matrix (18). Thus the full local interpolation $P_G^{(2)}$ for this transformation $J_G^{(2)}$ is given by

$$P_G^{(2)} = \frac{1}{8} \begin{bmatrix} -8A_{G:11}^{-1} A_{G:12} \\ \mathbb{1} & \mathbb{1} & 0 & 0 \\ \mathbb{1} & 0 & \mathbb{1} & 0 \\ 0 & \mathbb{1} & 0 & \mathbb{1} \\ 0 & 0 & \mathbb{1} & \mathbb{1} \end{bmatrix}. \tag{19}$$

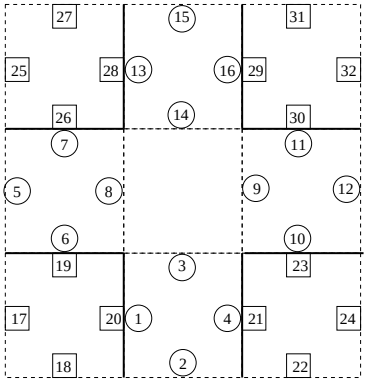

Figure 5: Degrees of freedom of reduced macro superelement

The fact that the static condensation step can be integrated in the (local) hierarchical basis transformation, which results in the local interpolation (19), can easily be seen if we multiply the two related matrices. Using the notation

$$P^{(16\times16)} = \frac{1}{8} \begin{bmatrix} \mathbb{1} & \mathbb{1} & 0 & 0 \\ \mathbb{1} & 0 & \mathbb{1} & 0 \\ 0 & \mathbb{1} & 0 & \mathbb{1} \\ 0 & 0 & \mathbb{1} & \mathbb{1} \end{bmatrix}$$

for the lower square (16×16) block of (19) those two consecutive steps result in the (combined) transformation

$$\begin{aligned} J_G^{(2)} &= \begin{bmatrix} I^{(4\times4)} & 0^{(4\times16)} & -A_{G:11}^{-1} A_{G:12}^{(4\times16)} \\ 0^{(16\times4)} & I^{(16\times16)} & 0^{(16\times16)} \\ 0^{(16\times4)} & 0^{(16\times16)} & I^{(16\times16)} \end{bmatrix} \begin{bmatrix} I^{(4\times4)} & 0^{(4\times16)} & 0^{(4\times16)} \\ 0^{(16\times4)} & I^{(16\times16)} & P^{(16\times16)} \\ 0^{(16\times4)} & 0^{(16\times16)} & I^{(16\times16)} \end{bmatrix} \\ &= \begin{bmatrix} I^{(4\times4)} & 0^{(4\times16)} & -A_{G:11}^{-1} A_{G:12}^{(4\times16)} \\ 0^{(16\times4)} & I^{(16\times16)} & P^{(16\times16)} \\ 0^{(16\times4)} & 0^{(16\times16)} & I^{(16\times16)} \end{bmatrix}. \end{aligned} \tag{20}$$

In other words, the (full) interpolation matrix, which is given by the upper right (20×16) block of the product (20) is the matrix (19).

In the third example, we combine the "First Reduce" step with a local harmonic interpolation of the remaining fine DOF subject to the constraint that the fine DOF of a given element are allowed to

interpolate only from the coarse DOF of its attached elements. Using Figure 5 for further explanation, this means that (in the scalar case) the DOF with local numbers $1, 2, 3, 4$ are allowed to interpolate from the coarse DOF with numbers $17, 18. \ldots, 24$ only. In order to construct a locally energy minimizing interpolation, we assemble an auxiliary matrix C_G from those face matrices that originally produce the coupling of the remaining fine DOF (local numbers 1 to 16) with the coarse DOF (local numbers 17 to 32). The corresponding faces are indicated by bold lines in Figure 5; Then, partitioning the matrix C_G into 2×2 blocks of size 16×16, i.e.,

$$C_G = \begin{bmatrix} C_{G:11} & C_{G:12} \\ C_{G:21} & C_{G:22} \end{bmatrix},$$

the transformation $J_G^{(3)}$ is defined by using the local interpolation

$$P_G^{(3)} = \begin{bmatrix} -A_{G:11}^{-1} A_{G:12} \\ -C_{G:11}^{-1} C_{G:12} \end{bmatrix}$$

in (17). Note that the nonzero pattern of the submatrix $-C_{G:11}^{-1} C_{G:12}$ is the same as that of the corresponding block of the matrix $P_G^{(2)}$! This ensures that the local stencil of the original (nodal basis) fine-grid matrix is reproduced on the coarse level(s).

We shall now briefly discuss the generalization of our approach to vector-field problems. In the simplest case, such as for the Lamé system of linear elasticity, nodes accumulate variables of the same kind, e.g., displacement components. As we have seen earlier, this may involve a "preprocessing step", such as the elimination of the "pressure unknowns", if one starts from a mixed formulation of the problem. Then, if we number (reorder) the DOF node-by-node (instead of component-by-component) the aforementioned procedure can be applied directly.

The face-stiffness matrices $\bar{A}_e^{\mathrm{h}}$ and $\bar{A}_e^{\mathrm{v}}$ with respect to the node-by-node ordering are obtained from the matrices (13) and (14) via the following permutation of rows and columns:

$$\bar{A}_e^{\mathrm{h}} = S_{\mathrm{c,n}}^t A_e^{\mathrm{h}} S_{\mathrm{c,n}}, \quad \bar{A}_e^{\mathrm{v}} = S_{\mathrm{c,n}}^t A_e^{\mathrm{v}} S_{\mathrm{c,n}}, \tag{21}$$

where

$$\begin{aligned} (S_{\mathrm{c,n}})_{i,j} &= \begin{cases} 1 & \text{if} \quad j = \mathbf{s}_i \\ 0 & \text{else} \end{cases}, \\ \mathbf{s} &= (1, 3, 5, 7, 9, 11, 13, 15, 2, 4, 6, 8, 10, 12, 14, 16)^t. \end{aligned}$$

Now the two-level generalized hierarchical basis transformations that have been introduced in this section can be applied straightly using the face matrices (21). Only the doubling of the dimension of the respective vector spaces and hence of the corresponding matrix dimensions draws a natural distinction for this two-component system. In particular we will study the transformation variant $J_G^{(3)}$ for the Lamé system in the next section.

6 Numerical study of the CBS constant

The construction of optimal preconditioners in the framework of multilevel block factorization is based upon a theory in which the constant γ in the so-called strengthened Cauchy-Bunyakowski-Schwarz (CBS) inequality plays a key role. The CBS constant measures the cosine of the abstract angle between the coarse space and its complementary space. This splitting can be obtained implicitly via a generalized hierarchical basis transformation as described in the previous section. The value of the upper bound for $\gamma \in (0, 1)$ is also part of the construction of various multilevel extensions of the related two-level methods.

6.1 Local estimates of γ

In the hierarchical bases context we denote by $\mathcal{V}_1$ and $\mathcal{V}_2$ subspaces of the finite element space $\mathcal{V}_h$. The space $\mathcal{V}_2$ is spanned by the coarse-space basis functions and $\mathcal{V}_1$ is the complement of $\mathcal{V}_2$ in $\mathcal{V}_h$, i.e., $\mathcal{V}_h$ is a direct sum of $\mathcal{V}_1$ and $\mathcal{V}_2$:

$$\mathcal{V}_h = \mathcal{V}_1 \oplus \mathcal{V}_2$$

We want to emphasize that instead of computing the coarse-space basis functions explicitly, a (generalized) hierarchical basis can always be defined (implicitly) by specifying the related hierarchical basis transformation. The fact that we construct the global transformation based on a compatible local transformation ensures that the coarse-space basis functions have a local support; Actually, even the stencil, i.e., the sparsity pattern, of the original stiffness matrix (with respect to the standard nodal basis) is reproduced by the resulting coarse-level matrix that serves as a Schur complement approximation.

Let us consider the scalar second-order elliptic problem now. We first note that the following well-known definition of the strengthened CBS inequality constant

$$\gamma = \cos(\mathcal{V}_1,\, \mathcal{V}_2) = \sup_{u \in \mathcal{V}_1,\ v \in \mathcal{V}_2} \frac{\mathcal{A}(u,v)}{\sqrt{\mathcal{A}(u,u)\mathcal{A}(v,v)}}$$

holds where $\mathcal{A}(\cdot,\cdot)$ is the bilinear form that appears in the IP-DG finite element formulation (4). As it was shown in [2], the constant γ can be estimated locally, in our case over each macro superelement G, which means that $\gamma = \max_G \gamma_G$, where

$$\gamma_G = \sup_{u \in \mathcal{V}_1(G),\ v \in \mathcal{V}_2(G)} \frac{\mathcal{A}_G(u,v)}{\sqrt{\mathcal{A}_G(u,u)\mathcal{A}_G(v,v)}}, \quad v \neq \text{const}.$$

The spaces $\mathcal{V}_k(G)$ above contain the functions from $\mathcal{V}_k$ restricted to G and $\mathcal{A}_G(u,v)$ corresponds to $\mathcal{A}(u,v)$ restricted over the macro superelement G. We stress here, that the above technique has been developed originally for conforming finite elements; However, it can also be applied successfully to DG-nonconforming approximations if one uses the construction of overlapping macro superelements, see Section 5. Moreover, and this is demonstrated with the example of the Lamé system of linear elasticity here, the proposed approach is not limited to scalar problems.

The local analysis of the CBS constant is based on the following simple general rule to compute γ_G, see, e.g., [12, 20]:

$$\gamma_G^2 = 1 - \mu_1,$$

where μ_1 is the minimal eigenvalue of the generalized eigenproblem

$$S_G \mathbf{v}_{G:2} = \mu \hat{A}_{G:22} \mathbf{v}_{G:2}, \qquad \mathbf{v}_{G:2} \notin \ker(\hat{A}_{G:22}). \tag{22}$$

Here $\hat{A}_{G:22}$ denotes the lower-right block of the hierarchical macro-superelement matrix (16) obtained via either of the transformations $J_G^{(m)}$, $m \in \{1,2,3\}$. In case of the scalar elliptic problem $\hat{A}_{G:22}$ is of size 16×16 and its one-dimensional kernel is spanned by the constant vector, i.e.,

$$\ker(\hat{A}_{G:22}) = \text{span}\{(1,1,\ldots,1)^t\}.$$

In case of the Lamé system $\hat{A}_{G:22}$ is of size 32×32 (in two space dimensions) with a three-dimensional kernel spanned by the rigid body motions (2 translations and 1 rotation), i.e.,

$$\ker(\hat{A}_{G:22}) = \text{span}\{\mathbf{t}_1, \mathbf{t}_2, \mathbf{r}_1\}$$

where

$$\begin{aligned}\mathbf{t}_1 &= (1,0,1,0,\ldots,1,0)^t,\\ \mathbf{t}_2 &= (0,1,0,1,\ldots,0,1)^t,\\ \mathbf{r}_1 &= (-y_1,x_1,-y_2,x_2,\ldots,-y_{16},x_{16})^t\end{aligned}$$

and (x_i, y_i), $1 \le i \le 16$, are the coordinates of the coarse nodes of the macro superelement G. The matrix S_G denotes the local Schur complement, i.e.,

$$S_G = \hat{A}_{G:22} - \hat{A}_{G:21}(\hat{A}_{G:11})^{-1}\hat{A}_{G:12}.$$

It is easily seen that the minimal eigenvalue of (22) can be computed equivalently from

$$(V_G^t \hat{A}_{G:22} V_G)^{-1}(V_G^t S_G V_G)\mathbf{v}_{G:2} = \mu \mathbf{v}_{G:2}$$

where V_G is a matrix of size 16×15 for the scalar problem and of size 32×29 for the 2D elasticity problem and the columns of V_G are orthogonal to $\ker(\hat{A}_{G:22})$.[2]

6.2 Multilevel behavior of γ

The background of this work are multilevel methods that are based on a recursive application of certain two-level methods. Here we investigate robustness issues for particular splittings of certain DG-nonconforming approximations. As the classical theory predicts, efficient two- and multilevel preconditioners can be constructed based on such splittings if the CBS-constant γ is uniformly bounded away from 1. Considering the particular splittings that have been presented in Section 5 the numerical experiments described in the rest of this section are devoted to the verification of this important property.

In the first experiment we compute recursively the squared local CBS constant γ_G^2 for the scalar elliptic problem with constant coefficients. Each time the lower-right 16×16 block of the matrix $\hat{A}_G$ in (16) is used to assemble a new macro superelement matrix A_G that can be associated with the next coarser level then. Figure 6 depicts the multilevel behavior, i.e., the value of γ_G^2 on the first 15 levels for all three transformation variants. It is interesting to see that for the transformations $J_G^{(1)}$ and $J_G^{(2)}$ the recursive splitting results in a sequence of monotonically decreasing local γ-values as the recursion proceeds. On the other hand, γ_G first decreases then increases and finally converges to the same limit from above for $J_G^{(3)}$. In both cases, however, it is evident that the angle between the two subspaces is uniformly bounded from below. Of course, the sequence of recursively computed local γ-values depends on the choice of the stabilization parameter α in general. The results plotted in Figure 6 are for $\alpha = 10$.

The results in Figure 7 show the effect of increasing α, which leads to a steeper decrease of γ_G^2 (variant $J_G^{(3)}$) on the first few coarse levels. However, the CBS constant converges to $\sqrt{3/8}$ for any reasonable choice of α, e.g., for $\alpha > (\sqrt{23329} - 127)/8$, cf. Remark 3.1. It is already very close to its limit for any $\alpha \ge 10$ after 7 steps of recursion, see Figure 7.

A similar behavior can be observed for the Lamé system of linear elasticity if ν is fixed. While the limit of γ_G^2 seems to vary only slightly when varying the stabilization parameter α, it clearly depends on the Poisson ratio ν for this problem. The results plotted in Figure 8 are for $\nu = 0.33$.

[2] For instance, one can use all eigenvectors of $\hat{A}_{G:22}$ that correspond to all its nonzero eigenvalues to define the columns of V_G.

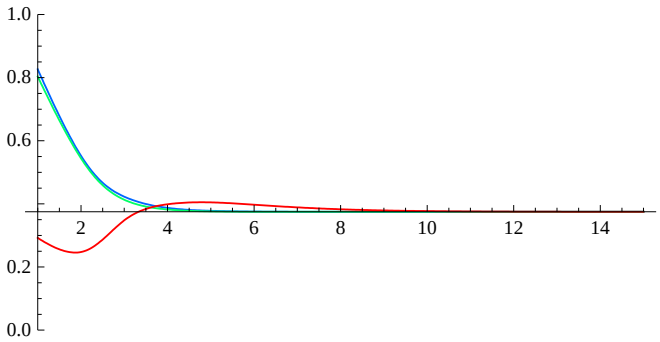

Figure 6: Multilevel behavior of γ_G^2 – scalar elliptic problem ($\alpha = 10$) – variant $J_G^{(1)}$ (blue curve); $J_G^{(2)}$ (green curve); $J_G^{(3)}$ (red curve)

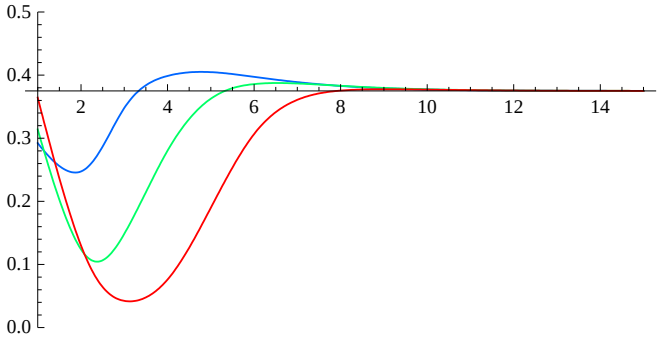

Figure 7: Multilevel behavior of γ_G^2 – scalar elliptic problem – variant $J_G^{(3)}$: $\alpha = 10$ (blue curve); $\alpha = 100$ (green curve); $\alpha = 1000$ (red curve)

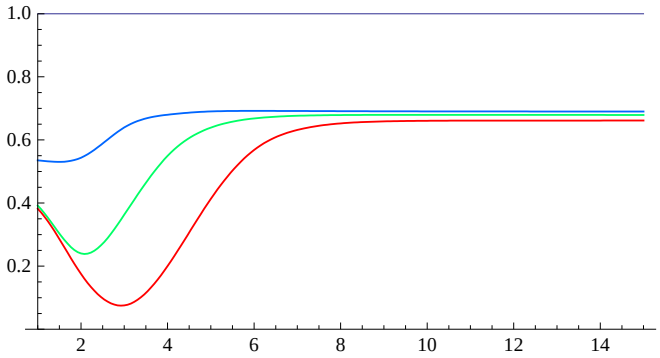

Figure 8: Multilevel behavior of γ_G^2 – elasticity problem ($\nu = 0.33$) – variant $J_G^{(3)}$: $\alpha = 10$ (blue curve); $\alpha = 100$ (green curve); $\alpha = 1000$ (red curve)

The dependence of γ_G^2 on the Poisson ratio is depicted in Figures 9 and 10 for $\alpha = 10$ and $\alpha = 1000$, respectively. We consider the transformation based on local harmonic interpolation, which yields the best results, again. Unfortunately, the splitting is not robust with respect to ν in the sense that γ_G^2 is not uniformly bounded away from 1 as the recursion proceeds. By comparing Figures 9 and 10, we see that an increase of α indeed improves the angle between the two subspaces, however, for almost incompressible materials, i.e., for ν being close to $1/2$, we observe that γ_G^2 approaches 1 on very coarse levels. Nevertheless, for a moderate Poisson ratio, i.e., for $\nu \leq 0.4$, the squared local CBS constant does not exceed $\sqrt{3/4}$ provided α is taken large enough. Thus according to the theory, we may conclude that a preconditioner with optimal order, i.e., $\mathcal{O}(1)$, condition number can be constructed based on W-cycle algebraic multilevel iteration (AMLI).

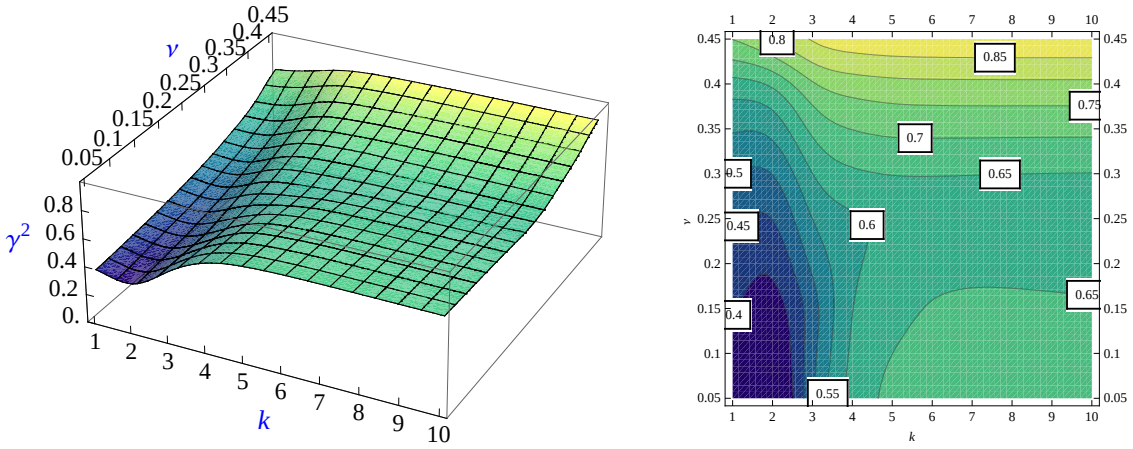

Figure 9: Multilevel behavior of γ_G^2 – elasticity problem; varying ν: $\alpha = 10$

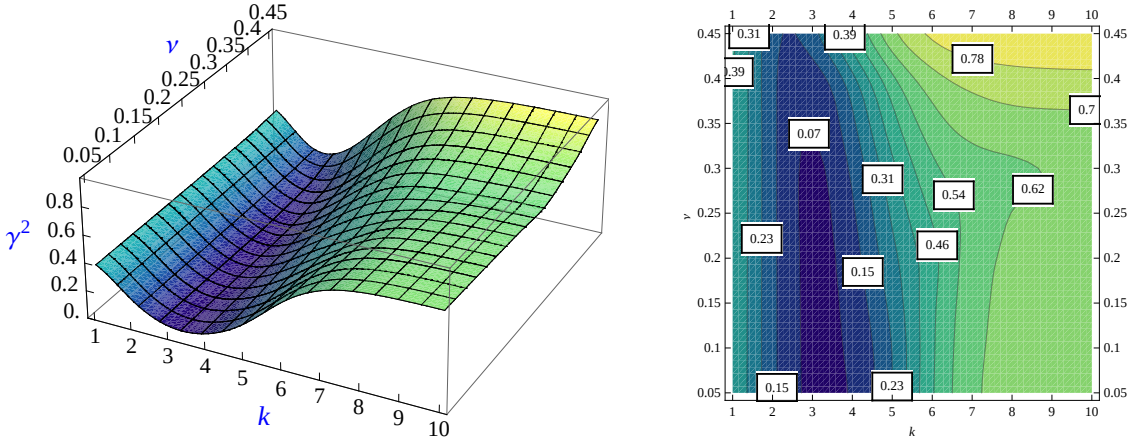

Figure 10: Multilevel behavior of γ_G^2 – elasticity problem; varying ν: $\alpha = 1000$

Note that W-cycle AMLI, which involves second-degree matrix polynomials for the stabilization of the condition number (or, alternatively, two inner iterations) at every coarse (except the coarsest)

level, can be performed at a cost proportional to N, the total number of DOF, per (outer) iteration in the present setting since the coarsening ratio τ is close to four, cf. Figure 4. If then, as we may predict from our results, the convergence factor of the preconditioned conjugate gradient method is strictly less than 1 independent on the number of levels, the overall solution process will be of optimal order of computational complexity. That is, the linear system can be solved up to any fixed (prescribed) accuracy at a total cost of $\mathcal{O}(N)$ arithmetic operations.

6.3 Random coefficients

In the following experiment we compute the value of the squared local CBS constant γ_G^2 for the case of random jumps in the coefficients on the macro superelement for different choices of the stabilization parameter α, i.e., $\alpha \in \{10, 100, 1000\}$. Again, the computations are carried out for the splitting based on static condensation and local harmonic interpolation, as described in Section 5.

The configuration is a stochastically independent uniformly distributed random value of the diffusion coefficient in the interval $(0, 1)$ for each element, i.e., a set of nine random numbers in $(0, 1)$ for the (reference) super macroelement. Then 100 randomly generated sets of random coefficients are generated and γ_G^2 is evaluated thrice for each such set, once for each choice of α. The results in Figure 11 show that the local CBS constant is always nicely bounded away from 1. However, its mean value $\bar{\gamma}_G^2$ and its variation both depend on α. The variation is smaller for larger α in general. Since $\bar{\gamma}_G^2$ is smaller for $\alpha = 100$ than it is for $\alpha = 10$ or for $\alpha = 1000$ it seems that minimizing the mean value of γ_G^2 requires some optimal (not too large) stabilization parameter.

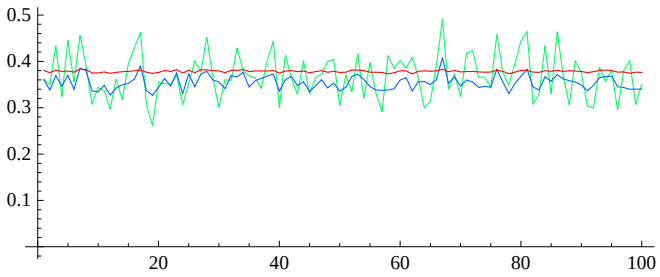

Figure 11: γ_G^2 for random coefficients: charts for $\alpha = 10$ (green), $\alpha = 100$ (blue), $\alpha = 1000$ (red)

Finally we discuss the results of a similar experiment for the Lamé system of linear elasticity. Here we choose a random Young's modulus E and let the Poisson ratio fixed, i.e., $\nu = 0.33$, which corresponds to a jump of the same relative magnitude of both Lamé parameters. We evaluate γ_G^2 for $\alpha \in \{10, 100, 1000\}$, again for 100 random distributions of E. As we see from Figure 12, the increase of α has almost no smoothing effect on the local CBS constant in this case.

7 Acknowledgments.

The authors gratefully acknowledge the support by the Austrian Academy of Sciences. They also express their gratitude to Prof. Raytcho Lazarov for his numerous advises and comments on the topic of DG methods.

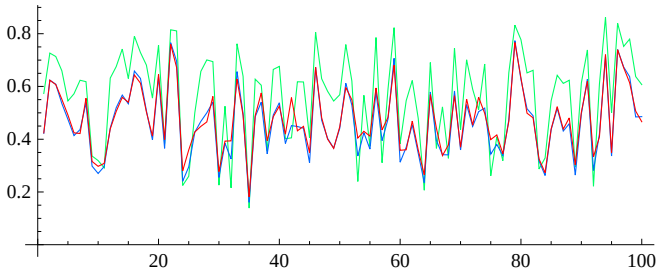

Figure 12: γ_G^2 for elasticity problem ($\nu = 0.33$) – random coefficients: charts for $\alpha = 10$ (green), $\alpha = 100$ (blue), $\alpha = 1000$ (red)

References

[1] D.N. Arnold and F. Brezzi, Mixed and non-conforming finite element methods: implementation, postprocessing and error estimates, *RAIRO, Model. Math. Anal. Numer.*, **19** (1985), 7-32.

[2] O. Axelsson and I. Gustafsson, Preconditioning and two-level multigrid methods of arbitrary degree of approximations, *Math. Comp.*, **40** (1983), 219-242.

[3] D. Arnold, F. Brezzi, B. Cockburn and L.D. Marini, Unified analysis of discontinuous Galerkin methods for elliptic problems, *SIAM J. Numer. Anal.*, **39** (2002), 1749–1779.

[4] O. Axelsson and P.S. Vassilevski, Algebraic Multilevel Preconditioning Methods I, *Numer. Math.*, **56** (1989), 157-177.

[5] O. Axelsson and P.S. Vassilevski, Algebraic Multilevel Preconditioning Methods II, *SIAM J. Numer. Anal.*, **27** (1990), 1569-1590.

[6] R. Blaheta, S. Margenov and M. Neytcheva, Uniform estimate of the constant in the strengthened CBS inequality for anisotropic non-conforming FEM systems, *Numer. Lin. Alg. Appl.*, **11(4)** (2004), 309-326.

[7] R. Blaheta, S. Margenov and M. Neytcheva, Robust optimal multilevel preconditioners for non-conforming finite element systems, *Numer. Lin. Alg. Appl.*, **12(5-6)** (2005), 495-514.

[8] S. Brenner and J. Zhao, Convergence of multigrid algorithms for interior penalty methods, *Appl. Numer. Anal. Comput. Math.*, **2(1)** (2005), 3-18.

[9] B. Cockburn, Discontinuous Galerkin methods, *Z. Angew. Math. Mech.*, **83(11)** (2003), 731-754.

[10] V.A. Dobrev, R.D. Lazarov, P.S. Vassilevski and L.T. Zikatanov, Two-level preconditioning of discontinuous Galerkin approximations of second order elliptic equations, *Numer. Lin. Alg. Appl.*, **13(6)** (2006), 753-770.

[11] V.A. Dobrev, R.D. Lazarov and L.T. Zikatanov, Preconditioning of symmetric interior penalty discontinuous Galerkin FEM for elliptic problems, *Domain Decomposition Methods in Science and Engineering XVII, Springer LNCSE*, **60** (2008), 33-44.

[12] V. Eijkhout and P.S. Vassilevski, The Role of the Strengthened Cauchy-Bunyakowski-Schwarz Inequality in Multilevel Methods, *SIAM Review*, **33** (1991), 405-419.

[13] R.E. Ewing, J. Wang, and Y. Yang, A stabilized discontinuous finite element method for elliptic problems, *Numer. Lin. Alg. Appl.*, **10(1-2)** (2003), 83-104.

[14] R. Falgout, P.S. Vassilevski and L.T. Zikatanov, On two-grid convergence estimates, *Numer. Lin. Alg. Appl.*, **12** (2005), 471-494.

[15] I. Georgiev, J. Kraus and S. Margenov, Multilevel preconditioning of 2D Rannacher-Turek FE problems; Additive and multiplicative methods, *Large–Scale Scientific Computing, Springer LNCS*, **4310** (2007), 56-64.

[16] I. Georgiev, J. Kraus and S. Margenov, Multilevel preconditioning of rotated bilinear nonconforming FEM problems, *Computers & Mathematics with Applications*, to appear. (Published Online: 20 Feb 2008, DOI: 10.1016/j.camwa.2007.11.008)

[17] J. Gopalakrishnan and G. Kanschat, A multilevel discontinuous Galerkin method, *Numerische Mathematik*, **95(3)** (2003), 527-550.

[18] P. Hansbo and M. Larson, A simple nonconforming bilinear element for the elasticity problem, *Trends in Computational Structural Mechanics, CIMNE*, (2001), 317-327.

[19] T.J.R. Huges, The Finite Element Method: Linear Static and Dynamic Finite Element Analysis, Prentice-Hall, New Jersey, 1987.

[20] J. Kraus, S. Margenov, Multilevel methods for anisotropic elliptic problems, *Lectures on Advanced Computational Methods in Mechanics, Radon Series Comp. Appl. Math.*, **1** (2007), 47-87.

[21] J. Kraus, S. Margenov, J. Synka, On the multilevel preconditioning of Crouzeix-Raviart elliptic problems, *Num. Lin. Alg. Appl.*, to appear. (Published Online: 31 Aug 2007, DOI: 10.1002/nla.543)

[22] J. Kraus and S. Tomar, Multilevel preconditioning of elliptic problems discretized by a class of discontinuous Galerkin methods, *SIAM J. Sci. Comput.*, to appear.

[23] J. Kraus and S. Tomar, A multilevel method for discontinuous Galerkin approximation of three-dimensional anisotropic elliptic problems, *Num. Lin. Alg. Appl.*, to appear. (Published Online: 16 Jul 2007, DOI: 10.1002/nla.544)

[24] R.D. Lazarov and S.D. Margenov, CBS constants for multilevel splitting of graph-Laplacian and application to preconditioning of discontinuous Galerkin systems, *Journal of Complexity*, **23** (2007), 498-515.

[25] R. Rannacher and S. Turek, Simple non-conforming quadrilateral Stokes Element, *Numerical Methods for Partial Differential Equations*, **8(2)** (1992), 97-112.